Thermochimica Acta, 53 (1982) 215–223
Elsevier Scientific Publishing Company, Amsterdam—Printed in The Netherlands

THERMAL DECOMPOSITIONS OF FORMATES. PART VII. THERMAL DECOMPOSITION OF YTTRIUM FORMATE DIHYDRATE

YOSHIO MASUDA

General Education Department, Niigata University, Niigata 950-21 (Japan)

(Received 11 September 1981)

ABSTRACT

The thermal dehydration of yttrium formate dihydrate and decomposition of yttrium formate anhydride were studied in flowing nitrogen and carbon dioxide atmospheres by means of TG and DTA.

The dehydration reaction was not affected by the atmospheric condition and took place successively without any intermediate hydrate. The mechanism of the dehydration reaction was found to be a phase boundary controlled interface reaction.

The decomposition of yttrium formate occurred in three stages, and yttrium oxyformate and yttrium oxycarbonate were formed as the intermediate products.

In a carbon dioxide atmosphere, the decomposition took place at a higher temperature than in a nitrogen atmosphere.

The anhydrous salt melted during the main stage of the decomposition and the kinetic behaviour of this stage was characteristic of a homogeneous first order reaction.

INTRODUCTION

Although thermal decompositions of metal formates have been extensively investigated in recent years, the thermal decomposition of yttrium formate is scarcely reported [1,2]. There has been some previous work on its decomposition, however, they do not seem to have described the thermal behavior of this salt, particularly with respect to its intermediate products.

In this study, the thermal decomposition of yttrium formate dihydrate in flowing nitrogen and carbon dioxide atmospheres was studied by the methods of thermogravimetry (TG) and differential thermal analysis (DTA) in the temperature range of 300–1200 K, and the stoichiometry of it was examined. In addition to this, the decomposition mechanism was discussed using the kinetic data obtained for the dehydration and decomposition.

EXPERIMENTAL

$Y(HCO_2)_3 \cdot 2H_2O$ (99.9%) was purchased from Kishida Chemical Co. Ltd., Japan. The dried sample was pulverized with a pestle and sieved to narrow fraction 275–325 mesh size.

0040-6031/82/0000–0000/$02.75 © 1982 Elsevier Scientific Publishing Company

TG and DTA curves were simultaneously recorded on a Rigaku Thermoflex TG-DTA M8075 at a heating rate of 5 K min^{-1}, in flowing N_2 and CO_2 atmospheres (flow rate: 90 cm^3 min^{-1}). About 10 mg of sample was weighed into a platinum crucible and measured using α-alumina as a reference material.

Infrared absorption (IR) spectra of samples heated to various temperatures were measured from 250 to 4000 cm^{-1} in a KBr disc with a Hitachi 295 spectrophotometer, and X-ray powder diffraction patterns of those samples were obtained with a Rigaku Geigerflex diffractometer. Cu-Kα radiation and a nickel filter were used in all measurements.

Evolved gaseous products of decomposition were collectd in syringes at intervals of 2 min from 473 to 1200 K, and 2 cm^{-1} of each gas collected were analyzed with a Shimadzu GC-3BT gas chromatograph [3,4].

RESULTS AND DISCUSSION

Thermal analysis of dehydration of $Y(HCO_2)_3 \cdot 2\,H_2O$

TG and DTA curves of $Y(HCO_2)_3 \cdot 2\,H_2O$ in flowing N_2 and CO_2 atmospheres are shown in Fig. 1. The temperature range for the dehydration of $Y(HCO_2)_3 \cdot 2\,H_2O$, the temperature for the peak of DTA curve and the weight loss after complete dehydration are listed in Table 1.

The smoothness of the curves and agreement between the calculated and observed

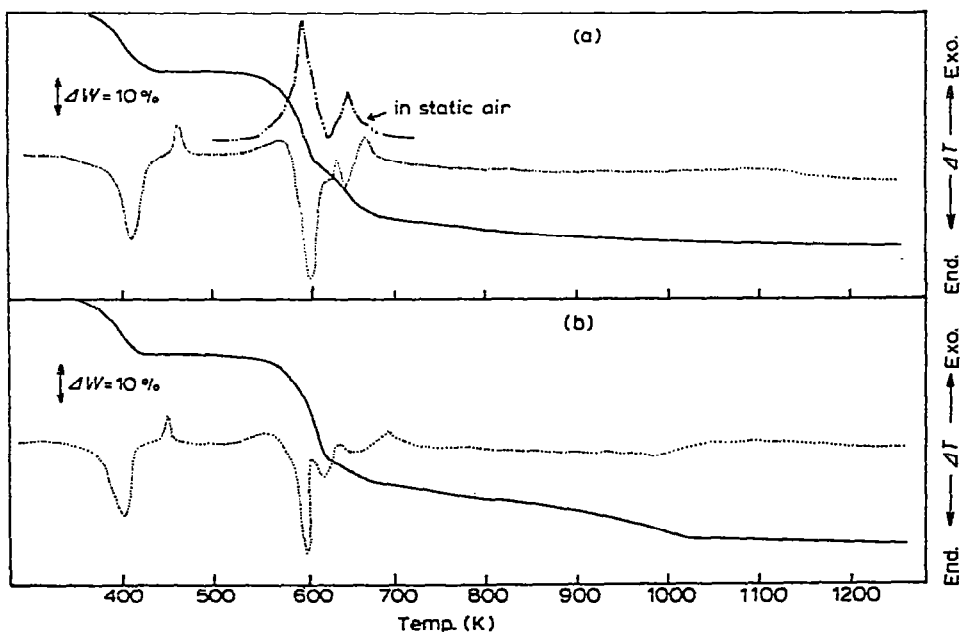

Fig. 1. TG (solid line) and DTA (broken line) for the thermal decomposition of $Y(HCO_2)_3 \cdot 2\,H_2O$. (a) In nitrogen; (b) in carbon dioxide.

TABLE I

Temperature range, temperature for peak of DTA curve (Tp) and weight loss value for dehydration

Atmosphere	Temperature range (K)	Tp (K)	Weight loss (%)	
			Calcd.	Obsd.
N_2	353–413	394	13.9	14.1
CO_2	354–414	393	13.9	13.5

values of weight loss, suggest that the dehydration takes place successively without any intermediate hydrate. The temperature range for dehydration and the peak temperature of the DTA curve in both atmospheres were almost equal, therefore the dehydration reactoin was little affected by the atmospheric condition.

Thermal analysis of $Y(HCO_2)_3$

In a nitrogen atmosphere

After the dehydration, an exothermic peak was found at 455 K in the DTA curve, but the weight loss corresponding to this process was not found. X-Ray powder diffraction patterns and IR spectra of solid residues obtained before and after this exothermic peak were measured to elucidate what phenomena or change corresponded to this peak. The sample A obtained almost immediately after dehydration was poorly crystalline, on the other hand, the X-ray pattern of sample B heated to 473 K showed a rhombohedral crystal structure [1,5,6]. In addition, A gives a broad

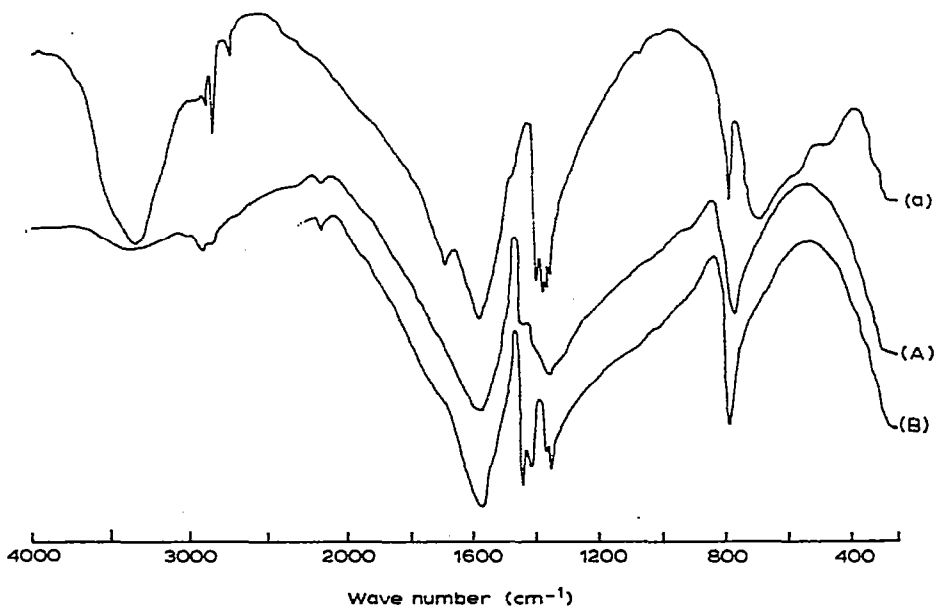

Fig. 2. IR spectra of $Y(HCO_2)_3 \cdot 2\,H_2O$ (a) and $Y(HCO_2)_3 \cdot 2\,H_2O$ heated to 413 K (A) and 473 K (B).

IR band at around 1360 cm^{-1}, while B gives sharp bands which are assigned to symmetric CO stretching (1360 cm^{-1}) and C–H bending (1420 and 1445 cm^{-1}) (Fig. 2) [2.7–9]. These results suggest that the exothermic peak is attributed to the recrystallization of amorphous yttrium formate anhydride.

The decomposition process of $Y(HCO_2)_3$ seemed to be divided into three stages (Table 2). The first stage occurred in the range of 523–613 K with a weight loss of 28.0%. An endothermic peak which had a shoulder at the high temperature side was observed at 596 K. The microscopic observation of $Y(HCO_2)_3$ at elevated temperatures showed that the specimen melted during decomposition in this temperature range. Therefore, this endothermic peak must be formed by the overlapping of the two peaks corresponding to melting and decomposition.

The pattern of the DTA curve for this stage was strongly affected by the atmospheric conditions. In static air, an exothermic peak appeared which was probably due to the combustion of the carbon monoxide and hydrogen produced on the decomposition (Fig. 1). In the CO_2 atmosphere the shoulder mentioned above shifted to a higher temperature and two endothermic peaks appeared.

Gas analysis showed that the decomposition involved almost simultaneous evolution of H_2 and CO_2 at 553 K and that of CO at 573 K. The composition of gaseous products in this stage were H_2, 35%; CO, 25% and CO_2, 40%. The ratio of these gaseous products varied as each decomposition stage proceeded (Fig. 3).

The residue at this stage was poorly crystalline and had an apparent composition of $YO(HCO_2)$. The brown colour of this residue which was due to the dispersed carbon, suggested the disproportionation of carbon monoxide

$$2\,CO \rightarrow CO_2 + C$$

A slight and broad exotherm recognized at around 530 K is probably due to this exothermic disproportionation.

The second stage of the decomposition occurred with an endothermic peak at 627 K. The residue at this stage is poorly crystalline, but the IR spectrum of it shows distinct bands at 1560, 1750 and 1380 cm^{-1} which agreed with those reported by Goldsmith and Ross [10] for yttrium oxycarbonate, $Y_2O_2CO_3$ (Fig. 4). The dark

TABLE 2

Thermal decomposition of $Y(HCO_2)_3$

Atmosphere	Stage of decomposition	Temperature range(K)	T_p*(K)	Weight loss (%)	
				Calcd.	Obsd.
N_2	1st	523– 613	596	28.5	28.0
	2nd	613– 773	627	5.8	7.0
	3rd	773–1053		8.6	9.3
CO_2	1st	538– 633	597, 611	28.5	27.4
	2nd	633– 815	644	5.8	6.7
	3rd	815–1113		8.6	8.9

* Temperature for peak of DTA curve for each stage.

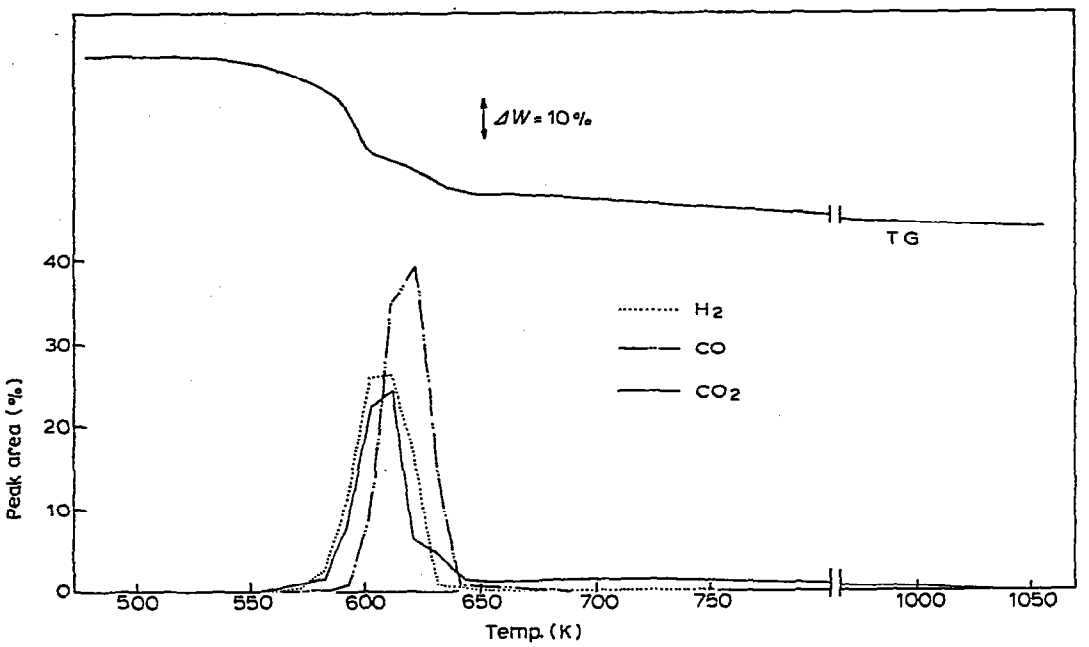

Fig. 3. Evolved H_2, CO and CO_2 on thermal decomposition of $Y(HCO_2)_3$ in nitrogen atmosphere.

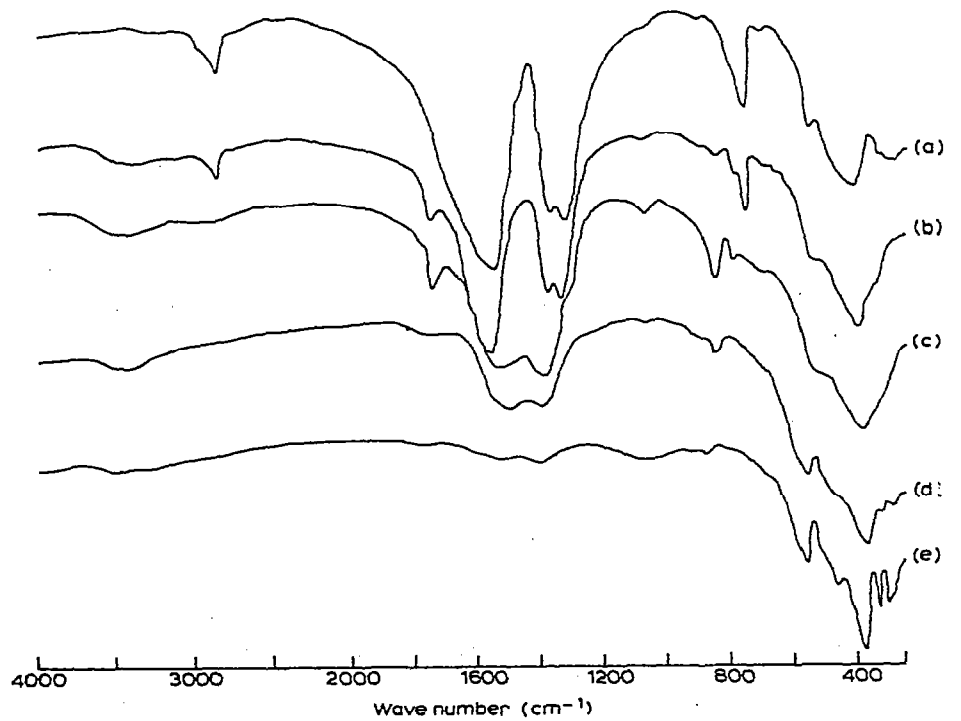

Fig. 4. IR spectra of $Y(HCO_2)_3$ heated to (a) 603 K, (b) 613 K, (c) 636 K, (d) 923 K and (e) 1123 K.

brown colour of the residue suggests the disproportionation of carbon monoxide.

The composition of the gaseous products in the second stage was H_2, 53%; CO, 38% and CO_2, 8%. The ratio of H_2 evolved in the first stage to that in the second stage was 1.9 : 1. These main gases contained small amounts of CH_4 and other organic compounds which were probably formed by a secondary reaction of the main gaseous products [16].

The third stage occurred very slowly without any clear endotherm and the weight loss level after this stage corresponded to the formation of Y_2O_3, which was confirmed by the X-ray diffraction pattern [11] and IR spectrum [10,12–15]. The IR spectra of the samples heated to 923 and 1123 K indicated that the $Y_2O_2CO_3$ was transformed to Y_2O_3 (Fig. 4). The gaseous product at this stage was only CO_2.

Based on the above experimental results, the following scheme is proposed for each stage of the decomposition of $Y(HCO_2)_3$ in a N_2 atmosphere

$$Y(HCO_2)_3 \rightarrow YO(HCO_2) + H_2 + CO_2 + CO \quad \text{(1st stage)}$$

$$2\,YO(HCO_2) \rightarrow Y_2O_2CO_3 + H_2 + CO \quad \text{(2nd stage)}$$

$$Y_2O_2CO_3 \rightarrow Y_2O_3 + CO_2 \quad \text{(3rd stage)}$$

In a carbon dioxide atmosphere

In a flowing CO_2 atmosphere, the decompositon took place at a higher temperature and proceeded more sluggishly compared with that in a N_2 atmosphere. The process of decomposition was divided into three stages (Table 2).

It is noteworthy that the endothermic peak observed at 596 K in a N_2 atmosphere was split into two endothermic peaks observed at 597 and 611 K. The first peak corresponds to melting and the second one to decomposition of the sample. The splitting of these peaks can be related to the depression of the first stage decomposition in a CO_2 atmosphere.

From the weight loss value and the elemental analysis of the residue, the intermediate product formed in the first stage was regarded as $YO(HCO_2)$. The thermal stability of this compound in a CO_2 atmosphere was confirmed by the IR spectrum of the solid residue. The IR spectrum of the sample heated to 803 K in CO_2 shows a broad band at around 2900 cm^{-1} which is assigned to C–H stretching [7–9]. On the other hand, this band is no longer detectable at 773 K in a N_2 atmosphere.

Although an intermediate product of composition $MO(HCO_2)$ was found in the thermal decomposition of rare earth formates [6], the formation of $YO(HCO_2)$ has not been reported. However the above experimental results provide evidence of it.

A distinct peak of the DTA curve for the third stage was not recognized, which may be due to the slow rate and low heat of reaction of this stage.

Based on the results obtained, the stoichiometry for the decomposition of $Y(HCO_2)_3$ in a CO_2 atmosphere was similar to those in a N_2 atmosphere.

Kinetics of dehydration

The kinetics of the dehydration were studied by the method described previously [17,18], and the kinetic parameters such as the order of reaction, activation energy and enthalpy change determined are listed in Table 3. The dehydration mechanism was found to be a phase boundary controlled interface reaction, which is similar to those of the other metal formate dihydrates.

Kinetics of decompositoin of anhydride

Many methods have been proposed to obtain the kinetic parameter from thermogravimetry [19–29]. In this study Ozawa's method [27], which considered the effect of heating rate, was used to determine the kinetic parameters for the main decomposition reaction of $Y(HCO_2)_3$. This method is similar to Doyle's method [21,22], but simpler.

Ozawa [27] showed that the plots of the logarithm of the heating rate versus the reciprocal of absolute temperature for a given weight loss value gave a straight line, the slope of which gave the activation energy (Table 4). By using the activation energy thus obtained, the weight changes are plotted against $\log\{(E/aR)p(E/RT)\}$, where E is the activation energy, a is the heating rate, R is the gas constant, T is the temperature and $p(E/RT)$ is the p function [21,22,27], and are compared with the theoretical thermogravimetric curves (Fig. 5). From these comparisons the mechanism of the decomposition of $Y(HCO_2)_3$ may be elucidated to be first order. It seems reasonable that the kinetic behaviour of the decomposition of $Y(HCO_2)_3$ which melted during the decomposition process was characteristic of a homogeneous first order reaction.

The activation energy for the main stage of decomposition in CO_2 is higher than that in a N_2 atmosphere (Table 4), which does not contradict the fact that the decomposition temperature in CO_2 is higher than in N_2. The decomposition in the solid or liquid state takes place when the partial pressure of the components of the solid or liquid becomes greater than the vapour pressure of the same component in the surrounding atmosphere, and the rate must be dependent on the difference in those two vapour pressures. Thus the slow decomposition in CO_2 may be explained

TABLE 3

Reaction order (n), activation energy (E), frequency factor (A) and enthalpy change (ΔH) for dehydration

Atmosphere	n	E (kJ mole^{-1})		A(min^{-1})	ΔH(kJ mole^{-1} ***)
		F-C *	Isothermal **		
N_2	0.63	115	119	1.1×10^{17}	115
CO_2	0.71	118	114	8.5×10^{16}	

* Freeman Carroll method.

** Isothermal method.

*** ΔH was measured in a static air atmosphere.

TABLE 4

Activation energy(E) and frequency factor(A) for the first stage of decomposition of $Y(HCO_2)_3$

Atmosphere	E(kJ mol^{-1})	A(min^{-1})
N_2	146	1.0×10^{12}
CO_2	173	2.7×10^{14}

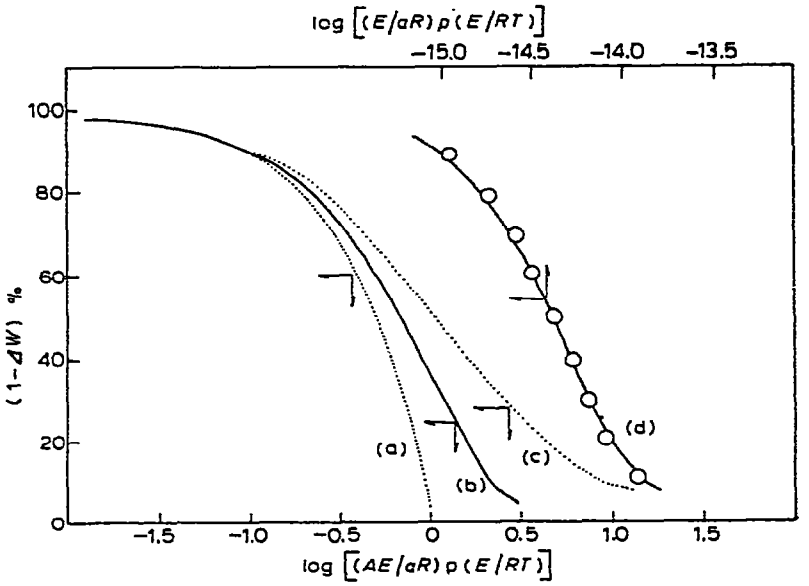

Fig. 5. The theoretical thermogravimetric curves for (a) zeroth-order reaction, (b) first-order reaction and (c) second-order reaction. Curve (d) is the experimental curve in a carbon dioxide atmosphere.

on the above basis, including the stabilization of the intermediate products by the CO_2 atmosphere.

ACKNOWLEDGEMENT

The author is grateful to Prof. Dr. Yuroku Yamamoto of Hiroshima University for his valuable advice.

REFERENCES

1 V.E. Plyshchev, L.P. Shklover, L.M. Shkol'nikova, G.P. Kuznetsova and T.A. Trushina, J. Gen. Chem. U.S.S.R., 35 (1965) 1781.
2 F.L. Carter, F. von Batchelder, J.F. Murray and P.H. Klein, Proc. 9th Rare Earth Res. Conf., Vol. II. 1972, p. 752.
3 S. Shishido and Y. Masuda, Nippon Kagaku Kaishi, (1976) 66.

4 Y. Masuda and S. Shishido, J. Inorg. Nucl. Chem., 42 (1980) 299.
5 V.E. Plyshchev, L.P. Shklover and L.M. Shkol'nikova, J. Struct. Chem. U.S.S.R., 7 (1966) 678.
6 R.P. Turcotte, J.M. Haschke, M.S. Jenkins and L. Eyring, J. Solid State Chem., 2 (1970) 593.
7 V.B. Kartha and T.S. Sugandhi, Indian J. Phys., 50 (1976) 115.
8 O.D. Saralidze, L.P. Shklover, K.I. Petrov and V.E. Plyshchev, J. Struct. Chem. U.S.S.R., 8 (1967) 45.
9 J.T.M. Hosson, J. Inorg. Nucl. Chem., 37 (1975) 2350.
10 J.A. Goldsmith and S.D. Ross, Spectrochim. Acta Part A, 23 (1967) 1909.
11 V.B. Glushkova and A.G. Boganov, Izv. Akad. Nauk U.S.S.R. Ser. Khim., 7 (1965) 1131.
12 W.B.White and V.G. Keramidas, Spectrochim. Acta Part A, 28 (1972) 501.
13 N.T. McDevitt and W.L. Baum, Spectrochim. Acta, 20 (1964) 799.
14 O. Kammori, N. Yamaguchi and K. Sato, Bunseki Kagaku, 16 (1967) 1050.
15 F. Petru and A. Muck, Z. Chem., 6 (1966) 386.
16 S.Shishido and Y. Masuda, Nippon Kagaku Kaishi, (1973) 394.
17 Y. Masuda and S. Shishido, Thermochim. Acta, 28 (1979) 377.
18 Y. Masuda, Thermochim. Acta, 39 (1980) 235.
19 E.S. Freeman and B. Carroll, J. Phys. Chem., 62 (1958) 394.
20 D.A. Anderson and E.S. Freeman, J. Polym. Sci., 54 (1961) 253.
21 C.D. Doyle, J. Appl. Polym. Sci., 5 (1961) 285.
22 C.D. Doyle, J. Appl. Polym. Sci., 6 (1962) 639.
23 H.H. Horowitz and G. Metzger, Anal. Chem., 35 (1963) 1464.
24 A.W. Coats and J.P. Redfern, Nature (London), 201 (1964) 68.
25 H.C. Anderson, J. Polym. Sci., C6 (1964) 175.
26 H.L. Friedman, J. Polym. Sci., C6 (1964) 183.
27 T. Ozawa, Bull. Chem. Soc. Jpn., 38 (1965) 1881.
28 P.K. Chatterjee, J. Polym. Sci. Part A, 3 (1965) 4253.
29 J.H. Sharp and S.A. Wentworth, Anal. Chem., 41 (1969) 2060.